Spiral wave chimera states in regular and fractal neuronal networks

Journal of Physics: Complexity

OPEN ACCESS

PAPER

Spiral wave chimera states in regular and fractal neuronal networks

Moises S Santos[1], Paulo R Protachevicz[1,2], Iberê L Caldas[1,*], Kelly C Iarosz[3,4], Ricardo L Viana[5], José D Szezech Jr[2,6], Silvio L T de Souza[7] and Antonio M Batista[1,2,6]

[1] Instituto de Física, Universidade de São Paulo, 05508-900, São Paulo, SP, Brazil
[2] Graduate Program in Science-Physics, State University of Ponta Grossa, 84030-900, Ponta Grossa, PR, Brazil
[3] Faculdade de Telêmaco Borba (FATEB), 84266-010, Telêmaco Borba, PR, Brazil
[4] Graduate Program in Chemical Engineering, Federal Technological University of Paraná, Ponta Grossa, 84016-210, Ponta Grossa, PR, Brazil
[5] Department of Physics, Federal University of Paraná, 82590-300, Curitiba, PR, Brazil
[6] Department of Mathematics and Statistics, State University of Ponta Grossa, 84030-900, Ponta Grossa, PR, Brazil
[7] Federal University of São João del-Rei, Campus Centro-Oeste, 35501-296, Divinópolis, MG, Brazil
[*] Author to whom any correspondence should be addressed.

E-mail: ibere@if.usp.br

Keywords: spiral wave chimera, fractal, neuronal networks

RECEIVED
3 September 2020

REVISED
16 November 2020

ACCEPTED FOR PUBLICATION
23 November 2020

PUBLISHED
10 December 2020

Abstract

Chimera states are spatial patterns in which coherent and incoherent patterns coexist. It was reported that small populations of coupled oscillators can exhibit chimera with transient nature. This spatial coexistence has been observed in various network topologies of coupled systems, such as coupled pendula, coupled chemical oscillators, and neuronal networks. In this work, we build two-dimensional neuronal networks with regular and fractal topologies to study chimera states. In the regular network, we consider a coupling between the nearest neighbours neurons, while the fractal network is constructed according to the square Cantor set. Our networks are composed of coupled adaptive exponential integrate-and-fire neurons, that can exhibit spike or burst activities. Depending on the parameters, we find spiral wave chimeras in both regular and fractal networks. The spiral wave chimeras arise for different values of the intensity of the excitatory synaptic conductance. In our simulations, we verify the existence of multicore chimera states. The cores are made up of neurons with desynchronous behaviour and the spiral waves rotates around them. The cores can be related to bumps or spatially localised pulses of neuronal activities. We also show that the initial value of the adaptation current plays an important role in the existence of spiral wave chimera states.

1. Introduction

Spatial patterns of coexisting coherence and incoherence were observed in 1989 by Umberger *et al* [1] in a dispersively coupled chain of nonlinear oscillators. In 2002, Kuramoto and Battogtokh [2] noticed spatial patterns with coherent and incoherent domains in networks composed of oscillators described by the Ginzburg–Landau equations with nonlocal coupling topology. This kind of spatial pattern was called chimera by Abrams and Strogatz [3]. Wolfrum and Omel'chenko [4] demonstrated the transient nature [5] of small populations of chimera states.

Chimera states [6] have been found in many experimental settings, for instance, mechanical oscillator networks [7, 8], chaotic opto-electronic oscillators [9], oscillator circuits [10], and coupled chemical oscillators [11]. Mukhametov *et al* [12] reported that synchronous and desynchronous behaviour can appear simultaneously or independently in the two brain hemispheres of dolphins.

The existence of chimera states was observed in theoretical and numerical studies [13], such as networks of Kuramoto oscillators [14], coupled Landau–Stuart equations [15], and Belousov–Zhabotinsky oscillators [16]. Hizanidis *et al* [17] identified chimera in a network of Hindmarsh–Rose neurons coupled according to

the connectome of the *Caenorhabditis elegans* soil worm. Batista *et al* [18] found chimera states in coupled maps and chaotic systems by using a local form of the order parameter.

For the studies about chimera states, networks with different topologies have been considered. It was reported that chimera states emerge in local, nonlocal, and global coupling topologies [19]. In 2019, Argyropoulos and Provata [20] provided numerical evidence of the coexistence of coherent and incoherent domains in two-dimensional network with fractal connectivity. A fractal is a geometric structure that exhibits self-similarity and its dimension has non integer value. They found spiral wave chimeras and triple coexistence of coherent domains, incoherent regions and travelling waves. Spiral wave chimeras were theoretically proposed in 2004 by Shima and Kuramoto [21] by means of a nonlocally coupled oscillators. Gu *et al* [22] observed spiral wave chimeras in locally chaotic homogeneous systems under nonlocal coupling. The chimeras were characterised by synchronisation defect lines separating domains of different oscillation phases. The union between spiral wave dynamics and chimera states can be found in chemical and biological systems [23]. Totz *et al* [24] reported an experimental verification of spiral wave chimera in chemical micro-oscillators. They carried out experiments with catalyst-loaded ion-exchange beads in a catalyst-free Belousov–Zhabotinsky reaction mixture.

Recent research has been demonstrated the importance of chimera states in neuronal systems [25]. Wang *et al* [26] found chimera in an adaptive neuronal network with burst-timing-dependent plasticity. They showed different evolution of the chimera states due to the plasticity. We build a network composed of adaptive exponential integrate-and-fire (AEIF) neurons. The AEIF model was proposed by Brette and Gerstner [27] to describe neuronal activity. The AEIF model has an exponential and an adaptation mechanisms. Naud *et al* [28] reported that the AEIF is capable of generating multiple firing patterns, such as initial bursting, regular bursting, tonic spiking, and continuous adaptation. They investigated the parameter space and found regions corresponding to the firing patterns. Touboul and Brette [29] identified a complex bifurcation structure and the existence of chaotic spike patterns. This way, the AEIF model can be used to reproduce qualitatively various electrophysiological features. Protachevicz *et al* [30] observed spiking and bursting synchronous behaviour in a network of coupled AEIF neurons based on the human cortico-cortical connections. Recently, considering a network of AEIF neurons, Protachevicz *et al* [31] demonstrated that a short delay in the conductance is relevant to avoid abnormal neuronal synchronisation. Chimera states were found in an AEIF neuronal network [32], in which the neurons were connected with their nearest neighbours. The observed chimera was composed of groups of neurons with spike and burst patterns. Experimental evidences of chimera states were reported in neuroscience, for instance in neuronal activities related to unihemispheric sleep [33] and pathological brain states [34]. Lainscsek *et al* [35] verified that cortical chimera can predict epileptic seizures. Bansal *et al* [36] studied cognitive chimera states in human brain networks.

The main goal of our study is to verify the existence of spiral wave chimera states in regular and fractal networks, in which the local dynamics is described by the AEIF neuron. The AEIF model is able to mimic known neuronal activities. We consider a two-dimensional network with regular coupling and another with fractal topology. In the network with fractal topology, the connections are given by the Cantor constructions algorithm for a fractal set [37]. Bassett *et al* [38] reported evidence of a fractal architecture in human brain functional networks in the resting state. In this work, we show the existence of spiral wave chimeras in both regular and fractal networks of coupled AEIF neurons, when the neurons have spike activities. Depending on the coupling strength and initial value of the adaptation current, the networks can exhibit multicore chimera states. The core reveals a set of desynchronised neurons that can be associated with neuronal bumps. Bumps in networks of spiking neurons [39] play an important role in working memory [40] and feature selectivity [41]. Laing [42] demonstrated that bumps can arise in small-world networks with coupled excitatory and inhibitory neurons. Recently, Schmidt and Avitabile [43] investigated conditions for the existence and stability of bumps in networks of spiking neurons.

This paper is organised as follows. Section 2 introduces the neuronal networks of coupled AEIF neurons, in which we consider regular and fractal couplings. In section 3, we show the existence of spiral waves chimeras for different values of the coupling strength and the initial adaptation current. In the last section, we draw our conclusions.

2. Adaptive exponential integrate-and-fire neuronal networks

We build two-dimensional networks composed of $N \times N$ AEIF neurons [27] that are coupled by means of chemical synapses. The AEIF model has an exponential mechanism and an adaptation equation. Depending on the parameters, it can exhibit spikes and bursts activities. In our two-dimensional networks, the neurons are connected to R nearest neighbours according to regular or fractal topologies. In our simulations, a network is not converted to another. In the network with regular topology, the neurons are connected with their nearest neighbours, while the fractal network has a topology generated by the Cantor constructions algorithm

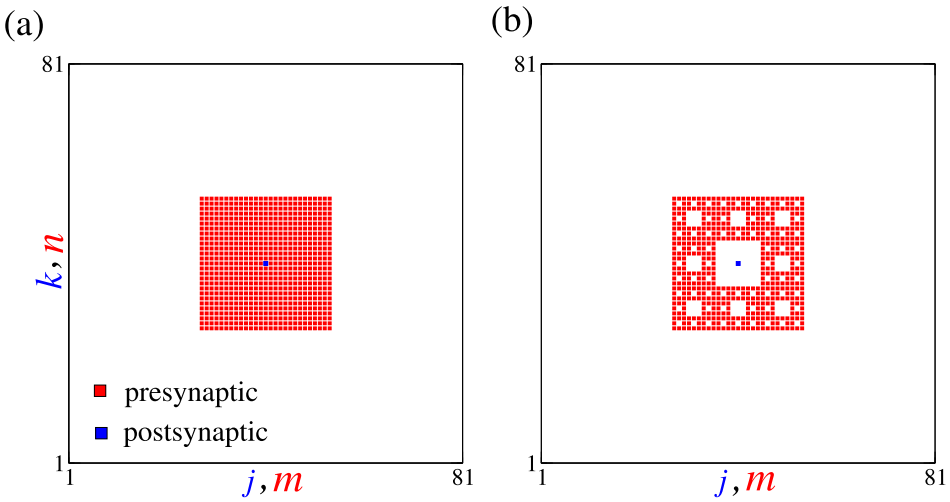

Figure 1. Two-dimensional coupling matrices of the (a) regular and (b) fractal networks for $N = 81$ and $R = 13$. The blue (j, k) and red (m, n) squares correspond to the postsynaptic and presynaptic neurons. The fractal topology is generated by means of the Cantor construction algorithm.

for a fractal set. Two-dimensional neuronal networks have been considered in research *in vitro*. Segev *et al* [44] presented measurements of spontaneous activities of cultured two-dimensional neuronal networks utilising a multielectrode array technique. Fractal arrangement of neuron axons in two-dimensional network was uncovered through tractography images produced by magnetic resonance imaging scans [45].

The neuronal network model is given by

$$\begin{aligned} C_{\mathrm{m}}\frac{\mathrm{d}V_{j,k}}{\mathrm{d}t} &= -g_{\mathrm{L}}(V_{j,k}-E_{\mathrm{L}}) + g_{\mathrm{L}}\Delta_{\mathrm{T}}\exp\left(\frac{V_{j,k}-V_{\mathrm{T}}}{\Delta_{\mathrm{T}}}\right) - w_{j,k} + I \\ &\quad + (V_{\mathrm{REV}}-V_{j,k})\sum_{m=j-R}^{j+R}\sum_{n=k-R}^{k+R} g_{m,n}M_{j,k,m,n}, \\ \tau_w\frac{\mathrm{d}w_{j,k}}{\mathrm{d}t} &= a(V_{j,k}-E_{\mathrm{L}}) - w_{j,k}, \\ \tau_{\mathrm{s}}\frac{\mathrm{d}g_{j,k}}{\mathrm{d}t} &= -g_{j,k}, \end{aligned} \tag{1}$$

where C_{m} is the membrane capacitance, $V_{j,k}$ is the membrane potential, g_{L} is the leak conductance, E_{L} is the resting potential, Δ_{T} is the slope factor, V_{T} is the spike threshold potential, $w_{j,k}$ is the adaptation current, I is the injection of current, V_{REV} is the synaptic reversal potential, and $g_{j,k}$ is the synaptic conductance. The adjacency matrix $M_{j,k,m,n}$ has elements with values equal to 1 when the presynaptic (m, n) and postsynaptic (j, k) neurons are connected, and 0 when they are unconnected. In our simulations, we consider $C_{\mathrm{m}} = 200$ pF, $E_{\mathrm{L}} = -70$ mV, $g_{\mathrm{L}} = 12$ nS, $\Delta_{\mathrm{T}} = 2$ mV, $V_{\mathrm{T}} = -50$ mV, $\tau_{\mathrm{w}} = 300$ ms, $a = 2$ nS, $\tau_{\mathrm{s}} = 1.5$ ms, $I = 500$ pA, $V_{\mathrm{REV}} = 0$ mV (excitatory synapses). When $V_{j,k} > V_{\mathrm{thres}}$ [28], $V_{j,k}$, $w_{j,k}$, and $g_{j,k}$ are updated following the rules

$$\begin{aligned} V_{j,k} &\to V_{\mathrm{r}}, \\ w_{j,k} &\to w_{j,k} + b, \\ g_{j,k} &\to g_{\mathrm{ex}}, \end{aligned}$$

where $V_{\mathrm{r}} = -58$ mV and $b = 70$ pA. g_{ex} is the maximal intensity of the excitatory synaptic conductance. The initial conditions of the neuronal potential and adaptation current are randomly chosen in the range $V_{j,k} = [-58, -38]$ mV and $w_{j,k} = [0, 70]$ pA, respectively. The initial conductance of each neuron $(g_{j,k})$ are considered equal to 0.

Figures 1(a) and (b) display the coupling matrices of the regular and fractal networks, respectively, for $N = 81$ neurons and $R = 13$. The fractal topology is generated by means of the Cantor construction algorithm [37]. The red squares denote the neurons that are connected to the central neuron (blue square) in the network. We consider periodic boundary conditions. In our simulations, to solve the differential equations, we use the Runge–Kutta 4th order method with step equal to 0.01 for 7000 ms and a transient time equal to 5000 ms.

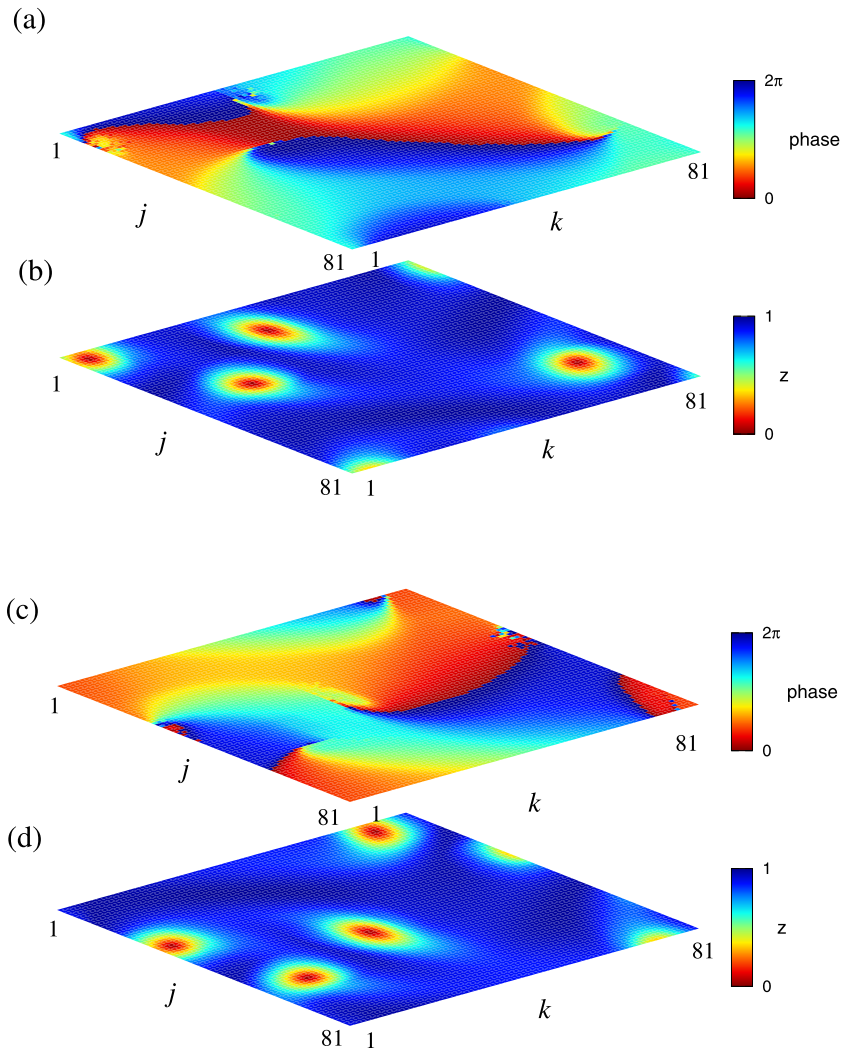

Figure 2. Spatial profiles of the phase and local order parameter z for the regular ((a) and (b)) and fractal ((c) and (d)) couplings, where we consider $g_{ex} = 0.042$ and $g_{ex} = 0.058$, respectively. In panels (b) and (d), the four red regions have small values of the local order parameter and correspond to the cores.

We utilise the two-dimensional local order parameter as a diagnostic tool to identify spiral wave chimera states, given by [24]

$$z_{j,k}(t) = \frac{1}{(2\delta+1)^2}\left|\sum_{m=j-\delta}^{j+\delta}\sum_{n=k-\delta}^{k+\delta} e^{i\phi_{m,n}(t)}\right|, \tag{2}$$

where $2\delta + 1$ is the side length of a square region with the neuron (j, k) in the center ($\delta = 4$). The phase is defined as

$$\phi_{j,k}(t) = 2\pi l + 2\pi\frac{t - t^l_{j,k}}{t^{l+1}_{j,k} - t^l_{j,k}}, \tag{3}$$

where $t^l_{j,k}$ is the time of the lth spike of the neuron (j, k), $t^l_{j,k} < t < t^{l+1}_{j,k}$, and the spike happens for $V_{j,k} > V_{\text{thres}}$.

We calculate the coefficient of variation of the inter-spike interval ($\text{ISI}_l = t^{l+1} - t^l$)

$$\text{CV} = \frac{\sigma_{\text{ISI}}}{\overline{\text{ISI}}}, \tag{4}$$

where σ_{ISI} is the standard deviation and $\overline{\text{ISI}}$ is the mean value of ISI. The spike and burst activities are characterised by CV < 0.5 and CV $\geqslant 0.5$, respectively [46].

3. Spiral wave chimera states

The spiral wave chimera states exhibit the coexistence of coherent and incoherent patterns in which an ordered spiral wave rotates around a core made up of desynchronous behaviour [24]. Figure 2 displays the spatial

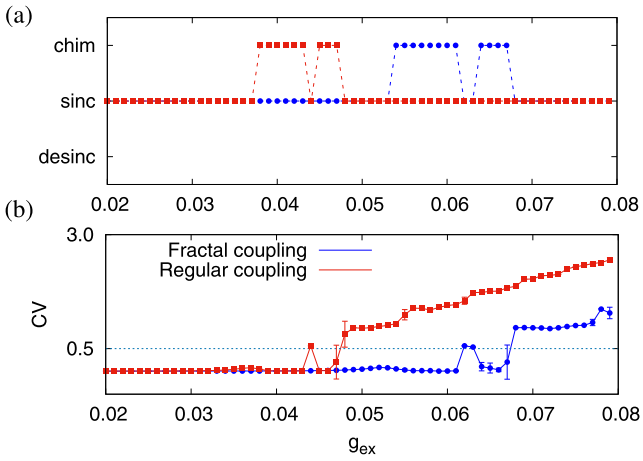

Figure 3. (a) Values of g_{ex} in which synchronous behaviour and spiral wave chimeras appear. (b) Coefficient of variation (CV) for 7 different initial conditions. The spiral wave chimeras occur in the range $0.02 \leqslant g_{ex} \leqslant 0.08$ in which the neurons have spike activities (CV < 0.5).

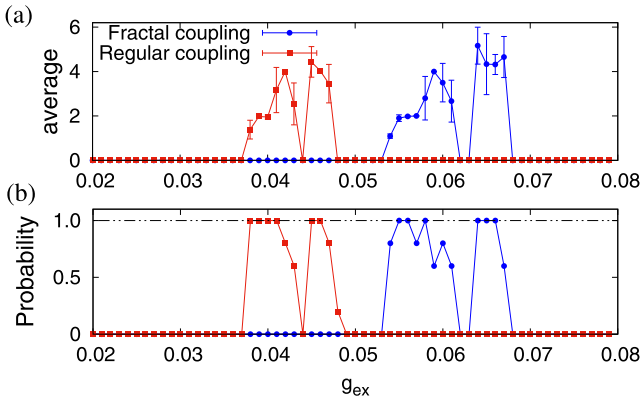

Figure 4. (a) Average and standard deviation of the number of cores. (b) Spiral wave chimera probability for different initial conditions as a function of g_{ex} for the regular (red squares) and fractal (blue circles) as a function of g_{ex} for fractal and regular couplings. Depending on the values of g_{ex}, different number of cores can arise in both regular and fractal networks.

profiles of the phase and local order parameter z for the regular (figures 2(a) and (b)) and fractal (figures 2(c) and (d)) networks. We observe the existence of spiral wave chimera for both regular and fractal couplings. In figures 2(b) and (d), the four red regions have small values of the local order parameter and correspond to the cores.

The spiral wave chimeras appear for different values of g_{ex} in the regular and fractal networks. Figure 3(a) displays two ranges of g_{ex} values for $g_{ex} \lesssim 0.048$ in which chimera states in the regular network (red squares) are observed. In the fractal network (blue circles), we find chimera for g_{ex} values larger than 0.048. In figure 3(b), we see that the networks can exhibit spike (CV < 0.5) and burst (CV $\geqslant 0.5$) activities. The transition from spikes to bursts of the fractal network after the regular network is due to its smaller number of connections. In our simulations, we observe that the spiral wave chimeras occur in the range $0.02 \leqslant g_{ex} \leqslant 0.08$ in which the neurons have spike activities (CV < 0.5).

Depending on the values of g_{ex}, different number of cores can arise in both regular and fractal networks. Figure 4(a) shows the average and the standard deviation of the number of cores as a function of g_{ex}. The cores exhibit desynchronous spike activities. By varying the initial conditions, we find a maximum of 5 and 6 cores for regular and fractal couplings, respectively. The multicores appear for values of g_{ex} smaller in the regular than in the fractal networks.

The existence of chimera depends on the system parameters and the initial conditions. The initial conditions play a crucial role in the emergence of chimera states [47]. In figure 4(b), we calculate the probability of the emergence of spiral wave chimeras for different initial conditions as a function of g_{ex}. For some g_{ex}, there is a set of initial conditions which goes to the chimera states. Due to this fact, we analyse the effects of different initial adaptation currents on the emergence of spiral wave chimeras.

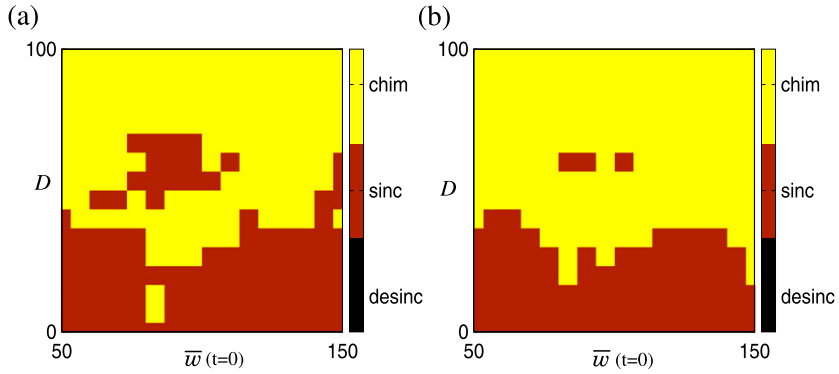

Figure 5. $D \times \overline{w}$ for the (a) regular ($g_{ex} = 0.0473$) and (b) fractal ($g_{ex} = 0.067$) networks, where values of $w_{j,k}$ are randomly distributed in the interval $\overline{w} - D \leqslant w_{j,k} \leqslant \overline{w} + D$. The spiral wave chimera, synchronised, and desynchronise states are denoted by yellow, red, and black colours, respectively.

Figure 5 displays $D \times \overline{w}$, where $\overline{w}$ is the mean of the initial adaptation currents and D is the range size of the distribution. The values of $w_{j,k}$ are randomly distributed in the interval $\overline{w} - D \leqslant w_{j,k} \leqslant \overline{w} + D$. The spiral wave chimera, synchronised, and desynchronise states are denoted by yellow, red, and black colours, respectively. Figure 5(a) is for the network with regular topology, while figure 5(b) is for the network with fractal topology. Depending on the values of D and $\overline{w}$, both networks exhibit chimera and synchronised states. In both topologies, spiral wave chimera states arise for $D > 70$. For intermediate values $40 \leqslant D \leqslant 70$, chimera and synchronised states depend on the topology. For $D < 40$, it is more difficult to find chimeras due to the fact that the initial adaptation currents are close, and as consequence the neurons synchronise. In our simulations (figure 5), we do not observe desynchronised patterns.

4. Conclusions

The coexistence of coherent and incoherent spatial patterns, known as chimera states, have been observed in several dynamics systems. They have appeared in different types of topologies. Spiral wave chimera states have been found in two-dimensional networks. These chimeras are characterised by spiral waves rotating around cores with desynchronous patterns.

In this work, we build networks composed of coupled AEIF neurons. Depending on the parameters, the AEIF neuron can exhibit spike or burst activities. We study the emergence of chimera states in networks with regular and fractal topologies. In the regular network, we consider a coupling between the nearest neighbours neurons, while the fractal network is constructed according to the square Cantor set.

We find spiral wave chimeras in both the networks for different values of the intensity of the excitatory synaptic conductance g_{ex}. According to the coefficient of variation, the neurons exhibit spike activities in the chimera states. We identify the existence of spiral wave chimeras with more than one core. The core reveals a set of desynchronised neurons that can be related to neuronal bumps. The bump states or spatially localised pulses of activities in coupled spiking neurons play an important role in working memory and visual orientation. The emergence of chimeras and the number of cores depend on the parameters and the initial conditions. We show that the initial adaptation currents are relevant for the appearance of spiral wave chimera states.

Data availability statement

All data that support the findings of this study are included within the article (and any supplementary information files).

Acknowledgments

This study was possible by partial financial support from the following Brazilian government agencies: Fundação Araucária, National Council for Scientific and Technological Development (CNPq), Coordenação de Aperfeiçoamento de Pessoal de Nível Superior-Brasil (CAPES), and São Paulo Research Foundation (FAPESP) (2018/03211-6, 2020/04624-2).

ORCID iDs

Antonio M Batista https://orcid.org/0000-0002-5899-0591

References

[1] Umberger D K, Grebogi C, Ott E and Afeyan B 1989 *Phys. Rev.* A **39** 4835–42
[2] Kuramoto Y and Battogtokh D 2002 *Nonlinear Phenom. Complex Syst.* **5** 380–5
[3] Abrams D M and Strogatz S H 2004 *Phys. Rev. Lett.* **93** 174102
[4] Wolfrum M and Omel'chenko 2011 *Phys. Rev.* E **84** 015201
[5] Lai Y-C and Tél T 2011 *Transient Chaos: Complex Dynamics on Finite Time Scales* vol 173(Berlin: Springer)
[6] Maistrenko Y L, Vasylenko A, Sudakov O, Levchenko R and Maistrenko V L 2014 *Int. J. Bifurcation Chaos* **24** 1440014
[7] Kapitaniak T, Kuzma P, Wojewoda J, Czolczynski K and Maistrenko Y 2014 *Sci. Rep.* **4** 6379
[8] Martens E A, Thutupalli S, Fourrière A and Hallatschek O 2013 *Proc. Natl Acad. Sci.* **110** 10563–7
[9] Hart J D, Bansal K, Murphy T E and Roy R 2016 *Chaos* **26** 094801
[10] Meena C, Murali K and Sinha S 2016 *Int. J. Bifurcation Chaos* **26** 1630023
[11] Tinsley M R, Nkomo S and Showalter K 2012 *Nat. Phys.* **8** 662–5
[12] Mukhametov L M, Supin A Y and Polyakova I G 1977 *Brain Res.* **134** 581–4
[13] Parastesh F, Jafari S, Azarnoush H, Shahriari Z, Wang Z, Boccaletti S and Perc M 2020 *Phys. Rep.* (in press)
[14] Santos M S, Szezech J D Jr, Batista A M, Caldas I L, Viana R L and Lopes S R 2015 *Phys. Lett.* A **379** 2188–92
[15] Omel'chenko O E, Maistrenko Y L and Tass P A 2008 *Phys. Rev. Lett.* **100** 044105
[16] Nkomo S, Tinsley M R and Showalter J 2013 *Phys. Rev. Lett.* **110** 244102
[17] Hizanidis J, Kouvaris N E, Zamora-López G, Díaz-Guilera A and Antonopoulos C G 2016 *Sci. Rep.* **6** 19845
[18] Batista C A S, Viana R L and Batista A M 2020 it Pramana (unpublished)
[19] Bera B K, Majhi S, Ghosh D and Perc M 2017 *Europhys. Lett.* **118** 10001
[20] Argyropoulos G and Provata A 2019 *Front. Appl. Math. Stat.* **5** 35
[21] Shima S and Kuramoto Y 2004 *Phys. Rev.* E **69** 036213
[22] Gu C, St-Yves G and Davidsen J 2013 *Phys. Rev. Lett.* **111** 134101
[23] Li B-W and Dierckx H 2016 *Phys. Rev.* E **93** 020202
[24] Totz J F, Rode J, Tinsley M R, Showalter K and Engel H 2018 *Nat. Phys.* **14** 282–5
[25] Majhi S, Bera B K, Ghosh D and Perc M 2019 *Phys. Life Rev.* **28** 100–21
[26] Wang Z, Baruni S, Parastesh F, Jafari S, Ghosh D, Perc M and Hussain I 2020 *Neurocomputing* **406** 117–26
[27] Brette R and Gerstner W 2005 *J. Neurophysiol.* **94** 3637–42
[28] Naud R, Marcille N, Clopath C and Gerstner W 2008 *Biol. Cybern.* **99** 335–47
[29] Touboul J and Brette R 2008 *Biol. Cybern.* **99** 319–34
[30] Protachevicz P R *et al* 2018 *Physiol. Meas.* **39** 074006
[31] Protachevicz P R *et al* 2020 *Front. Physiol.* **11** 1053
[32] Santos M S *et al* 2019 *Chaos* **29** 043106
[33] Rattenborg N C, Amlaner C J and Lima S L 2000 *Neurosci. Biobehav. Rev.* **24** 817–42
[34] Levy R, Hutchison W D, Lozano A M and Dostrovsky J O 2000 *J. Neurosci.* **20** 7766–75
[35] Lainscsek C, Rungratsameetaweemana N, Cash S S and Sejnowski T J 2019 *Chaos* **29** 121106
[36] Bansal K, Garcia J O, Tompson S H, Verstynen T, Vettel J M and Muldoon S F 2019 *Sci. Adv.* **5** eaau8535
[37] Sawicki J, Omelchenko I, Zakharova A and Schöll E 2019 *Eur. Phys. J.* B **92** 1–8
[38] Bassett D S, Meyer-Lindenberg A, Achard S, Duke T and Bullmore E 2006 *Proc. Natl Acad. Sci.* **103** 19518–23
[39] Laing C R and Chow C C 2001 *Neural Comput.* **13** 1473–94
[40] Wimmer K, Nykamp D Q, Constantinidis C and Compte A 2014 *Nat. Neurosci.* **17** 431–9
[41] Kim S S, Rouault H, Druckmann S and Jayaraman V 2017 *Science* **356** 849–53
[42] Laing C R 2016 *Front. Comput. Neurosci.* **10** 53
[43] Schmidt H and Avitabile D 2020 *Chaos* **30** 033133
[44] Segev R, Shapira Y, Benveniste M and Ben-Jacob E 2001 *Phys. Rev.* E **64** 011920
[45] Katsaloulis P, Verganelakis D A and Provata A 2009 *Fractals* **17** 181–9
[46] Borges F S, Protachevicz P R, Lameu E L, Bonetti R C, Iarosz K C, Caldas I L, Baptista M S and Batista A M 2017 *Neural Netw.* **90** 1
[47] Faghani Z, Arab Z, Parastesh F, Jafari S, Perc M and Slavinec M 2018 *Chaos, Solit. Fractals* **114** 306–11